JPET Fast Forward. Published on April 5, 2006 as DOI: 10.1124/jpet.105.098020

JPET #98020

Title:

A Selective p38α MAPK Inhibitor Reverses Cartilage and Bone Destruction in Mice with Collagen-Induced Arthritis

Authors:

Satyanarayana Medicherla, Jing Ying Ma, Ruban Mangadu, Yebin Jiang, Jenny J. Zhao, Ramona Almirez, Irene Kerr, Elizabeth G. Stebbins, Gilbert O'Young, Ann M. Kapoun, Gregory Luedtke, Sarvajit Chakravarty, Sundeep Dugar, Harry K. Genant and Andrew A. Protter

Institute:

Scios Inc, 6500 Paseo Padre Parkway

Fremont, CA-94555, USA (SM, JYM, RM, RA, IK, EGS, GO'Y, AMK, GL, SC, SD, AP)

Osteoporosis and Arthritis Research Group, UCSF, San Francisco, CA-94143 (YJ, JJZ, HKG)

Running title:

p38α MAPK Inhibitor Reverses Cartilage and Bone Destruction

Address of corresponding author:

Satyanarayana Medicherla

Scios Inc, 6500 Paseo Padre Parkway, Fremont, CA-94555, USA

Phone: **510-739-4311**

Fax: **510-739-4546**

Email: **medicherla@sciosinc.com**

Text : 23 pages

Tables : 3

Figures : 10

References : 40

Abstract: 204 words

Introduction: 355 words

Discussion: 316 words

Abbreviations:

BV/TV, bone volume/trabecular volume; CFA, complete Freund's adjuvant; CIA, collagen-induced arthritis; COMP, cartilage oligomeric matrix protein; COX, cyclooxygenase; ELISA, enzyme-linked immunosorbant assay; ICFA, incomplete Freund's adjuvant; IL, interleukin; IgG, immunoglobulin; LC, liquid chromatography; MAPK, Mitogen-Activated Protein Kinase; Micro-CT, μCT, micro-computed tomography; MS/MS, tandem mass spectrometry; PEG, propylene ethyl glycol; RA, rheumatoid arthritis; TNFα, tumor necrosis factor alpha;

ABSTRACT

Destruction of cartilage and bone are poorly managed hallmarks of human rheumatoid arthritis (RA). p38 mitogen activated protein kinase (p38MAPK) has been shown to regulate key pro-inflammatory pathways in RA, including TNF-alpha , IL-1beta, and COX 2, as well as the process of osteoclast differentiation. We therefore evaluated whether a p38-alpha MAPK inhibitor, SD-282, could modulate cartilage and bone destruction in a mouse model of RA induced with bovine type II collagen (collagen induced arthritis, CIA). In mice with early disease, SD-282 treatment significantly improved clinical severity scores, reduced bone and cartilage loss and reduced mRNA levels of pro-inflammatory genes in paw tissue including IL-1beta, IL-6 and COX- 2. Notably, SD-282 treatment of mice with advanced disease resulted in significant improvement in clinical severity scoring and paw swelling, a reversal in bone and cartilage destruction as assessed by histology, bone volume fraction and thickness, and 3-dimensional image analysis. These changes were accompanied by reduced osteoclast number and lowered levels of serum cartilage oligomeric matrix protein (COMP), a marker of cartilage breakdown. Thus, in a model of experimental arthritis associated with significant osteolysis, p38 alpha MAPK inhibition not only attenuates disease progression but also reverses cartilage and bone destruction in mice with advanced CIA disease.

INTRODUCTION

Cartilage and bone destruction are hallmarks of rheumatoid arthritic (RA) joints that are poorly managed by current therapeutic modalities. The therapeutic effectiveness of drugs that target either inflammatory cytokines such as TNFα and IL-1β or cyclooxygenase-2 (COX-2) have demonstrated the importance of these pathways on the pathology of the disease. p38 mitogen activated protein kinase (p38MAPK), an intracellular signaling protein, has been shown to regulate the expression of TNFα, IL-1β and COX2 and inhibitors of this kinase have demonstrated beneficial effects in animal models of arthritis (Kumar *et al.,* 2003; Nishikawa *et al.,* 2003). The roles of p38MAPK on bone and cartilage function suggest that inhibitors of this kinase may offer an important therapeutic benefit by modulating tissue destruction in RA patients.

In this paper, we describe the effect of SD-282, an alpha-specific inhibitor of p38MAPK, on bone and cartilage in a mouse model of collagen-induced arthritis (CIA). CIA in the mouse reproduces many aspects of the human disease, including joint inflammation, cartilage and bone destruction, and pannus accumulation (Williams *et al.*, 1992). Furthermore, inhibition of TNFα or IL-1β with antibodies has demonstrated beneficial effects in this preclinical model (Joosten *et al.,* 1999a) as well as in studies with RA patients. Osteolysis in mice with CIA is associated with increased joint osteoclasts (Suzuki, *et al.*, 1998) and p38MAPK plays an important role in osteolytic processes. p38MAPK regulates osteoclast differentiation induced by a wide variety of factors including PGE2, TNFα, G-CSF and RANK ligand (Li *et al., 2*002). In addition, p38MAPK inhibition blocks bone resorption in fetal rat long bone cultures *in vitro*

(Kumar *et al.,* 2001; Badger *et al.,* 1996) and prevent bone loss in isolated osteoblasts and bone marrow cells (Li *et al.,* 2002). FR167653 is an inhibitor of p38MAPK that, when used prophylactically, inhibits osteoclast numbers in rats with CIA (Nishikawa *et al.,* 2003). None of the studies addressed the role of specific or non-specific p38MAPK inhibitors on bone destruction in mice with an advanced state of CIA disease. Therefore, the effect of SD-282 on the osteolytic nature of joint lesions was evaluated by measuring bone destruction and osteoclast number in mice with advanced CIA disease.

MATERIALS AND METHODS

Animals: Male DBA-1 Lac/J mice were obtained from The Jackson Laboratory (Bar Harbor, ME) and the study was initiated when mice were 8 to 9 weeks of age.

Materials: Mouse diet (Lab Diet-5015) was from Deans Animal Feeds (San Carlos, CA). Complete Freund's adjuvant (CFA), incomplete Freund's adjuvant (ICFA) and *Mycobacterium tuberculosis* (strain H37Ra) were obtained from Difco Laboratories (Detroit, MI). Lipopolysaccharide (LPS) from *Escherichia coli*,0111:84 and acetic acid were purchased from Sigma (St. Louis, MO). Bovine type II collagen was purchased from University of Utah, (Salt Lake City, UT). Protease inhibitor cocktail was purchased from Roche (Indianapolis, IN), phosphatase inhibitor cocktail from Calibiochem (San Diego, CA), BCA assay kit from Pierce (Rockford, IL), antibodies for p38MAPK from Santa Cruz Biotechnology (Santa Cruz, CA), antibody for phospho-p38MAPK from Cell

Signaling Technologies (Beverly, MA) and Chemiluminescence ECL kit from Amersham. (Piscataway, NJ).

Chemical Description of SD-282: 282 is an indole-5-carboxamide, ATP-competitive inhibitor of p38 kinase. It is a small molecule, orally active inhibitor of p38α MAPK.

SD-282 Potency and Specificity: IC_{50} of SD-282 against the human p38MAPKs (α, β, γ, δ isoforms) were performed in duplicate using ELISA assays adapted from published methods (Clerk and Sugden, 1998; Kumar *et al.*, 1997; Hale *et al*., 1999; Goedert *et al.*, 1997). Purified human recombinant (*E. coli*) p38MAP kinase isoforms were incubated with substrate (Myelin Basic Protein [MBP], 10.75 μg/mL) in the presence of inhibitor or control in a buffer comprised of 50 mM Hepes, 20 mM $MgCl_2$, 0.2 mM Na_3VO_4, 1 mM DTT, pH 7.4 for 60 minutes at 25 C. The readout was ELISA quantitation of incorporation of ATP into MBP (MDS Pharma, Tampa, FL). Enzyme concentrations were as follows: 75 ng/mL p38α, 250 ng/mL p38β, p38γ, and p38δ . ATP concentration has been previously optimized for each assay and was 100 μM in the p38α assay, 10 μM in the p38β assay, 1 μM in the p38γ assay, and 3 μM in the p38δ assay. The control for the alpha and beta isoforms was SB 202190 and for the gamma and delta isoforms the control was staurosporine. The IC_{50} values of SD-282 for p38α MAPK were derived from two studies. As previously reported (Li *et al.*, 2004; Sweitzer *et al*., 2004), SD-282 demonstrates 14.3 fold selectivity for p38α MAPK (IC50 values of 0.0016 and 0.0011 μM) compared to p38β MAPK (IC50 values of 0.023 and 0.022 μM), whereas inhibition of p38γ MAP kinase and p38δ MAP kinase was less than

50% even at concentrations of 10 μM (Table I). When tested *in vitro* at a concentration of 10 μM, SD-282 demonstrated no inhibitory activity against a panel of other kinases including ERK2, JNK-1 and MAPKAPK-2. In addition, SD-282 demonstrates no effect on the activity of purified COX-1 or COX-2 enzymes.

Induction of arthritis in mice: Experimental arthritis was induced in mice with collagen and LPS treatments by the modified procedure of Joosten *et al.,* (Joosten, 1994 and 1997). Mice were immunized intradermally with bovine collagen II (100 μg) emulsified with *M. butyricum* in CFA (Difco Labs, Detroit, MN). On Day 21 the animals were boosted with an intradermal injection of 100 μg of collagen II dissolved in ICFA. On Day 23 animals received LPS (50 μg) intraperitoneally.

Clinical assessment of arthritis in mice: In this and subsequent studies, assessments were made by observers blinded to specimen identity and treatment, and to time-of-treatment. Mice paws were examined for disease severity and macroscopic scores were assigned as previously described (Williams, *et al.*, 1992). The clinical severity of arthritis was graded on a scale of 0 - 3 for each paw, according to changes in redness and swelling (0 = normal; 1 = slight swelling and erythema; 2 = pronounced edema; 3 = joint rigidity). Each limb was graded, resulting in a maximal clinical severity score of 12 per animal. The clinical severity score, number of paws affected and body weight were monitored daily during the entire study period. Paw swelling/volume was measured with reference to its baseline by plethysmography (Buxco; Wilmington, NC). Paws were

extracted for protein and p38MAPK and phospho-p38MAPK were detected by western blot

Western Blots: To prevent non-specific reaction with primary antibody, sections were pretreated with 5% normal donkey serum (Chemicon International, Inc, Temecula, CA) prior to IL-1β and IL-6 staining, or with 5% goat serum (Chemicon International, Inc, Temecula, CA) prior to COX-2 staining. After 3 washes with phosphate buffered saline (PBS), the sections were incubated with goat anti-mouse IL-1β (R&D System, Minneapolis, MN) at 1:100 and with goat anti-mouse IL-6 (R&D System, Minneapolis, MN) at 1:100 respectively at room temperature for 1 hour. Sections were incubated with rabbit anti-mouse COX-2 (ALEXIS, San Diego, CA) at 1:300 at room temperature for 1 hour. After 3 washes with PBS, the sections were incubated with donkey anti-goat biotinylated secondary antibody (Chemicon International, Inc., Temecula) for IL-1β and IL-6 staining at 1:2000 dilution at room temperature for 30 minutes. Sections were incubated with goat anti-rabbit biotinylated secondary antibody (Chemicon International, Temecula) for COX-2 staining at 1:2000 at room temperature for 30 minutes.

Treatment of animals with early stage disease: Two independent studies examined the effects of SD-282 treatment on the disease progression in animals with early stage CIA for a period of 10 days. In the first experiment, observation ended on Day 10. In the second experiment, SD-282 treatment was withdrawn on Day 10 and clinical severity scores were monitored for an additional 10 days. Mice with early signs of CIA (clinical severity score between 1 and 2) on Day 24 were treated twice daily by oral gavage (0.25 ml/animal, n=15 per treatment group) with 30 or 90 mg/kg of SD-282 or vehicle [1%

propylene ethyl glycol 400, (PEG)]. Clinical severity scores, paw swelling by plethysmography, and body weights were monitored. Paw tissues were evaluated for levels of p38MAPK, mRNA levels for IL-6, IL-1β, COX-2 and TNFα, and histologically. Paws close to the mean clinical severity scores were used for mRNA analysis (n =6) or p38MAPK analysis in joint tissue (n=9) or histology (n=15). Blood and paws from naïve mice (n=3 or 5) were also examined as necessary for data interpretation.

Treatment initiation in animals with advanced disease: Two independent experiments were conducted to evaluate the effect of SD-282 on cartilage and bone destruction in animals with advanced disease; each study had a control cohort treated with the vehicle alone (1% PEG). The first experiment examined the effect of 30 mg/kg and 90 mg/kg SD-282 doses for a period of 20 days, and the second experiment studied 90 mg/kg SD-282 for a period of 28 days. Mice with CIA clinical severity score between 9 and 10 on Day 30 (first experiment) or between 9 and 10 on ~Day 33 (second experiment) were either sacrificed for baseline data (n=6) or treated for 20 days (first experiment) or 28 days (second experiment) with SD-282 or vehicle as described above (n=12 per treatment group). Clinical severity scores, paw swelling by plethysmography, and body weights were measured in all animals. Paws were collected for histology and examination of the microstructure of the bone by 3-dimensional (3D) bone analysis. At the end of the second study, blood was saved for cartilage oligomeric matrix protein (COMP) determination.

Measurement of COMP: Murine COMP levels were determined in naïve (n=3), vehicle (n=12) and high dose groups (n=12) by AnaMar Medical (Uppsala, Sweden) by ELISA using similar conditions as described for the assay for human COMP (Saxne and Heinegard, 1992) and the assay details were reported earlier by Vingsbo-Lundberg and his colleagues (Vingsbo-Lunderber *et al.*, 1998).

Histological analysis of bone and cartilage destruction in CIA mice.

Tissue processing, sectioning and staining for histology: Paws were fixed, decalcified, processed and paraffin embedded longitudinally. Serial 5μm thick sections were cut at 250 μm intervals to reach the mid-paw region. At least six joints, including 2 small and 4 large joints, were observed at this orientation. Sections were stained with hematoxylin and eosin for histology or for immunohistochemistry (IL-1β, IL-6, or COX-2). After secondary antibody treatment, immunohistochemistry sections were treated with ABC reagents (Vector, Burlingame, CA) and then stained with diaminobenzidine (Invitrogen, Carlsbad, CA) and counterstained with hematoxylin. The same protocol was carried out for negative controls, in which the first antibody was omitted and an isotype-matched control antibody was used. The IL-1β, IL-6 and COX-2 immunohistochemical staining was analyzed for positive staining and scored on a scale of 0 to 4 for both intensity and for distribution. For intensity, no stain = 0, mild = 1, moderate = 2, strong = 3, strongest = 4. For distribution, none = 0, focal = 1, patchy = 2, diffuse = 3, strongly diffuse = 4. The overall score was a sum of intensity and distribution scores.

Tissue evaluation: Tissue was scored for cartilage and bone erosion, joint destruction, synovitis, pannus formation and synovial fibroplasia. Each parameter was scored as: 0- normal, 1- mild and one joint involved, 2- moderate and 2 joints involved, 3- moderately severe and 3 joints involved and 4- markedly severe damage and 4 or more joints involved. Quantitation of osteoclasts was performed by counting total number in each joint. A summary histological disease score for severity of arthritis was obtained by summation of all of the parameters.

Micro-CT 3-dimensional bone analysis: 3-D cortical and trabecular structural parameters, including bone volume fraction, thickness, and separation were measured without plate model assumption, in the distal radius and scaphoid, or in the distal tibia and the talus, after careful manual tracing the original periosteal surface.

µCT imaging acquisition: The front and rear paw specimens of the mice were examined using a cone-beam µCT scanner (µCT 40, Scanco Medical AG, Bassersdorf, Switzerland), with isotropic resolution of 16 um3. A scout view scan was obtained first for selection of the examination volume of the specimens, followed by positioning, measurement, and computational reconstruction (Jiang *et al.*, 2000).

Quantitative analysis of bone structure: From the original image analyses, we chose and analyzed a sub volume of containing the cortical bone and trabecular bone in the epiphysis and metaphysis of the distal tibia, the talus, distal radius, and the scaphoid. The volumetric data were divided by predetermined thresholds into binary data sets, and the bone tissue was

segmented from non-bone in the gray-value images with a fixed thresholding procedure for all samples. Parameters held constant included the filter width (Parfitt, 1983 and Jiang, *et al.*, in press), the filter support (2.0), and the threshold (27.5% of maximal possible gray value). 3-dimensional trabecular structural parameters were measured without stereological model assumptions, as previously described (Jiang,et.al.,2002, Takeshita, et.al., 2002). Mineralized bone was separated from bone marrow with a 3-D segmentation algorithm. The algorithm for separating mineralized bone from bone marrow was based on an analysis of the steepest gradient calculated from a continuous polynomial fit least-squares approximation of the originally discrete CT volume to find digital edges. Bone volume (BV) was calculated using tetrahedrons corresponding to the enclosed volume of the triangulated surface. Total volume (TV) was the volume of the sample that was examined. A normalized index, BV/TV, was used to compare samples of varying size. Bone structural thickness was estimated computationally by using the method of maximal spheres, and then calculating the average thickness of all bone voxels (volume-pixels). Bone structural separation was calculated with the same procedure as thickness, but the voxels representing non-bone parts were filled with maximal spheres (Takeshita, *et al.*, 2002).

Assessment of erosion: 3-D images of the front and rear paw specimens of the mice were reconstructed and displayed from different angles to examine the integrity of the bone surface. Bone erosion was graded with a method adapted from the Genant grading method (Genant *et al.*,1998). They were scored by 2 readers (JJZ and YJ), reaching a consensus when necessary by adopting a lower, more conservative score.

Bone erosion scoring: Erosion scoring was graded on a scale of 1 to 4 (0 = normal; 0.5 = subtle changes, 1 = mild, 1.5 = mild worse, 2 = moderate, 2.5 = moderate worse, 3 = severe, 3.5 = severe worse, 4.0=worst). In the frontal paw, 8 joints were examined: metacarpo-phalangeal of digits I to V, combination of all carpometacarpal and intercarpal joints, distal radius, and distal ulna. The maximum possible score was 28. In the rear paw, 14 joints were examined: bases of metatarsals I to V, cuneiforms I to III, cuboid, navicular, calcaneus, talus, distal fibula, and distal tibia. The maximum possible score was 56.

Statistical analysis:

Student's *t*-test or a non-parametric Mann-Whitney, or Bonferroni multiple comparison test wherever applicable, was used to determine a significant difference between vehicle and SD-282 treated groups. Differences were considered statistically significant when $p > 0.05$. All statistical analyses were done using Prism version 3.02 (GraphPad Software, San Diego, CA).

RESULTS

Collagen immunizations coupled with LPS treatment as a method to induce synovitis

reminiscent of human arthritis was originally developed by Joosten *et al.*, 1994 and 1997. In our hands and as shown below, early signs of disease (slight swelling and erythema in 1 to 2 paws) are first noted 24 days following the first immunization with collagen. At the time of initiation of the study when the clinical scores are in between 1 and 2 (i.e., day 24), p38αMAP kinase is present in joint tissue in an active state as judged by Western analysis, while not in tissue from non-diseased control animals (Figure 1). In general, it appears that mild phosphorylation of p38 levels correlate with a clinical score of 1 [Figure 1: lane 2 and 3], whereas moderate phosphorylatioin of p38 levels for paws correlate with clinical scores of 2 [Figure 1: lanes 1, 4 and 5]. Signs of the disease progressed and by Day 33 animals had pronounced swelling and erythema and joint rigidity in 3 to 4 paws. Histological assessment of mice at Day 33 revealed significant pannus, joint space narrowing and synovitis with IL-1 producing neutrophils and IL-6 producing monocyte macrophages present. In addition, osteoclasts were abundant and bone erosion and cartilage loss were prominent features of joint lesions. In the studies reported here, treatment was initiated in animals with early (Day 24) and advanced (Day 33) arthritis.

SD-282 attenuates CIA in mice with early stage disease.

Initiation of vehicle treatment of mice with early stage of the disease (mean clinical severity scores 1.6 ± 0.6 on Day 24) resulted in a progressive worsening of signs of disease, achieving a maximum clinical severity score of 7 ± 3.3 by Day 34. SD-282 treatment resulted in a dose-dependent improvement in clinical severity scores (Figure 2) and paw swelling as measured by plethysmometer. Swelling, expressed as mean percent

increase of paw size when compared to the baseline value, was 175%±100% for the vehicle-treated group, 90%±55% for animals treated with SD-282 at 30 mg/kg and 47%±43%* for animals treated with SD-282 at 90 mg/kg (*$p<0.001$ when compared to the vehicle group). SD-282 at 90 mg/kg treatment was also associated with a reduction mRNA levels for pro-inflammatory genes including IL-1β, IL-6 and COX-2 in paw tissue (Figure 3). Intriguingly, TNFα mRNA levels are very low in arthritic mouse paw tissues in the vehicle group at the end of the study. This precluded our ability to accurately assess the effect of SD-282 on TNFα at the end of the early stage treatment mode which falls on day 34, and which can be considered as advanced stage disease for untreated animals. This suggests that TNFα expression in the joint was not elevated in animals with advanced disease when compared to the naive healthy mice. TNFalpha mRNA levels were not significantly elevated at the time point used in this study consistent with previous reports showing no clear peak of TNF mRNA expression in the mouse CIA model (Rioja *et al.*, 2004).

Histological assessment of knee joints from vehicle treated animals showed clear evidence of synovitis with proliferating pannus, bone erosion, cartilage destruction and mononuclear cell infiltrate (Figure 4). There was little evidence of any inflammation or other disease-related changes including a loss in joint space in paw tissue from the SD-282-treatment group.

The effect of withdrawal of the p38αMAPK inhibitor on disease severity scores was evaluated in a second study. SD-282 treatment (30 and 90 mg/kg) when administered for

10 days from Day 25 to Day 35 resulted in a dose-dependent improvement in clinical severity scores as seen in the first study. At the time of treatment withdrawal [i.e., Day 35], clinical severity scores in vehicle, SD-282 30 mg/kg and SD-282 90 mg/kg groups were 9.7$\pm$ 1.6, 4.2$\pm$ 1.5 and 2.2$\pm$ 1, respectively. Cessation of SD-282 treatment from Day 35 onwards was not associated any further increase of clinical scores when mice were monitored for additional 10 days [i.e., up to day 44]. On Day 44, clinical severity scores in vehicle, SD-282 30 mg/kg and SD-282 90 mg/kg were 11$\pm$ 1, 4.4$\pm$ 1.6 and 2.2$\pm$ 1.2, respectively. This is a durable effect, as evidenced by steady clinical severity scores for up to 44 days of evaluation.

SD-282 reverses cartilage and bone destruction in mice with advanced disease.

In the first study, arthritic mice with advanced disease on Day 30 were treated for 20 days with vehicle or SD-282 (30 and 90 mg/kg b.i.d.) by oral gavage. At the time of treatment initiation, clinical severity scores in the vehicle, SD-282 30 mg/kg and SD-282 90 mg/kg groups were 9.1 ± 2.6, 9.0 ± 3.2 and 9.1 ± 2.6, respectively. SD-282 treatment was associated with a dose-dependent, statistically significant improvement in clinical severity scores (Figure 5) and paw swelling measured by plethysmometer. At the end of the treatment period clinical severity scores in the vehicle, SD-282 30 mg/kg and SD-282 90 mg/kg groups were 9.1 ± 2.2, 6.9 ± 1.6* and 4.9 ± 1.7**, respectively (*$p<0.05$, **$p<0.001$). Paw swelling at Day 50 (expressed as mean percent increase in paw size when compared to baseline) was 156%$\pm$16% in vehicle-treated animals, 142%$\pm$26% in animals treated with SD-282 at 30 mg/kg and 120%$\pm$16%* in animals treated with SD-282 at 90 mg/kg (*$p<0.01$ when compared to vehicle group). Cartilage and bone

destruction were evaluated by histology and 3-dimensional bone analysis. Histological assessment comparing tissue taken at the end of dosing from animals administered SD-282 or vehicle demonstrated a reversal in bone and cartilage destruction in the SD-282 treatment group (data not shown). The vehicle group demonstrated greater bone erosion and destruction (as assessed by 3-dimensional bone analysis) than did SD-282 treatment groups (Figure 6 A and B), consistent with increased bone resorption and heterotopic ossifications. Bone destruction was reversed as evidenced by the fact that bone volume fraction and thickness were statistically significantly greater in the SD-282 treated groups compared to the vehicle group (Table II). The 3-dimensional images show greater bone erosions and destruction because of increased bone resorption, and heterotopic ossifications in vehicle treated mice than in SD-282 treated mice.

To confirm the results of a prior study and to collect histological and bone data at the time of treatment initiation, a second study was performed. In this follow-up study, mice with signs of advanced disease (severity scores 9.6 ± 1.8, Day 33) were treated orally with vehicle or SD-282 at 90 mg/kg for 28 days, i.e. up to Day 61 . In the vehicle treatment group, clinical severity scores remained high through the end of the study (9.6 ± 1.8 and 9.3 ± 0.9 at the beginning and end of the treatment period, respectively). SD-282 treatment improved clinical severity scores in a statistically significant manner ($p<0.0003$) from a baseline of 9.5 ± 1.8 at the beginning of the study (Day 33) to 5.5 ± 2 by the end of the study (Day 61). SD-282 at 90 mg/kg also reduced paw swelling as measured by plethysmometer (data not shown). After 28 days of treatment, body weight

gain was higher in the SD-282 group compared to the vehicle group (4 $\pm$ 1 g and 2.8 $\pm$ 0.7 g, respectively; $p<0.01$).

In both experiments, cartilage and bone destruction were evaluated by histology. These two studies generated similar data on cartilage and bone destruction. Therefore, data in the second study is reported in this communication. To confirm that SD-282 has a key role in cartilage and bone destruction in joint disease, we graded pathology on sections of whole knee joints. In the naïve group, no abnormal histopathological changes were observed (Figure 7A). Histological examination of paw tissue from the baseline group revealed arthritic lesions clearly evident in both front and hind paws and in both small and large joints (Figure 7B). Histopathological changes including cartilage erosion, bone erosion, joint destruction, synovitis, pannus formation and synovial fibroplasia were observed in all of the examined paws. In the vehicle treated group at the end of the experiment (i.e., on Day 61), the development of arthritis was obvious in both front and hind paws and in both small and large joint (Figure 7C). Histopathological changes were observed in every one of the vehicle treated paws In contrast, for the SD-282 treated group, no markedly severe arthritis was observed in any of the paws (Figure 7D). Each of the six histolology parameters (cartilage, bone erosion, joint destruction, synovitis, pannus and fibroplasias) was lower in a statistically significant manner (Figures 8). In the vehicle treated group, osteoclasts (large multinuclear cells implicated in pathologic bone loss) were located at the site of bone destruction (arrows, Figure 9). Treatment with SD-282 significantly decreased the number of osteoclasts (1.5$\pm$1.5) when compared to the vehicle (6$\pm$2) at Day 61 (*$p<0.03$).

JPET Fast Forward. Published on April 5, 2006 as DOI: 10.1124/jpet.105.098020
This article has not been copyedited and formatted. The final version may differ from this version.

Immunohistochemistry of COX-2, IL-1β and IL-6: In the naïve group (no induction of arthritis and no treatment), COX-2, IL-1β and IL-6 were not observed in any sample by the staining methods used here. In the baseline group (representing time of treatment initiation after induction of arthritis), IL-1β staining was found in inflammatory cells (primarily neutrophils) within the joint area. IL-1β staining was significantly lower in the SD-282 group compared to the vehicle group ($p<0.02$, Figure 10 A1, B1 and C1; and Table III). IL-6 staining, primarily observed in macrophages, was low at baseline and was greater in the vehicle group than in the SD-282 group ($p<0.007$, Figure 10 A2, B2 and C2; and Table III). In the baseline group, COX-2 was detected in chondrocytes and synovial fibroblasts. At the end of the treatment period, COX-2 staining was significantly reduced in the SD-282 treatment group compared to the vehicle group ($p<0.01$, Figure 10 A3, B3 and C3; and Table III)

SD-282 reverses bone erosion in advanced CIA as evidenced by 3-dimensional μCT analysis: 3-dimensional μCT studies revealed a complete lack of bone erosion in samples from the naïve group. In contrast, bone erosion was significantly evident in the animals with CIA at baseline on Day 33. The erosion was more pronounced in the vehicle group on Day 61 (erosion score: 32 ± 15) than at baseline (erosion score: 12.7 ± 4.6). The erosion score of the SD-282-treated group at day 61 was 3.5 ± 2.9, apparently reversing erosion present at baseline, restoring the bone back to almost naïve levels ($p<0.0001$ when compared to the vehicle group). 3-dimensional μCT bone erosion scores show that the score in the vehicle group is about 2.5 fold over baseline, while the score in the SD-282

treatment group is over 9 fold lower than the vehicle group and about 3.5 fold lower than at baseline. 3-dimensional morphometric measurement shows that SD-282 treatment significantly reverses loss in the bone volume fraction and bone micro-architecture (data not shown).

Cartilage oligomeric matrix protein (COMP), a circulating marker of cartilage turnover is decreased by SD-282: To obtain further insight into the protection against cartilage destruction, we determined serum COMP levels in the naïve, vehicle and SD-282 groups of the second experiment. COMP is released from cartilage as a result of increased turnover in human and experimental arthritis. Circulating COMP levels were 2.1$\pm$0.4, 6.7$\pm$1 and 5.2$\pm$ 0.7 in naïve, vehicle and SD-282 at 90 mg/kg groups, respectively. SD-282 significantly reduced COMP levels when compared to the vehicle group ($p<0.001$).

DISCUSSION

Although the relative expression of p38MAPK isoforms in rheumatoid arthritis has not been fully explored, p38 α and δ MAPKs are known to be especially prevalent at sites of joint destruction (McLay et al, 2001). Here we show that at Day 24, an early phase of the disease, p38α MAPK is in an active (phosphorylated) state in tissue from arthritic joints compared with non-arthritic tissue. While we did not evaluate the phosphorylation state of p38α MAPK at time points later in the disease process, it is clear from histology that synovitis is present at Day 34 and Day 61 in animals with symptoms, suggesting p38α MAPK remains active in tissue from later disease stages. SD-282 demonstrated

selectivity for the α isoform, showing 14.3 to >1,000 times greater potency against p38αMAPK than it did against p38β-, p38γ- and p38δ-MAPKs. To further understand the role of the α isoform in arthritic disease and to explore the therapeutic potential of SD-282 on bone and cartilage destruction, we proceeded to test this α-specific inhibitor in mice with CIA disease. In particular, we were curious to see whether SD-282 would have beneficial effects in late stage disease, when bone and cartilage destruction become manifest.

It has been reported that a non-specific p38MAPK inhibitor attenuates arthritis in the early stage of the mouse CIA disease (Nishikawa *et al., 2*003). As expected from the anti-inflammatory profile of p38αMAPK inhibitors and previous studies in animals with experimental arthritis (Badger, *et al.,* 1996, Kumar *et al.*, 2003 and Nishikawa *et al.*, 2003), SD-282 treatment of animals with early stage arthritis reduced the progression of the disease. This effect was evidenced by improvements in clinical severity scores, histological assessments (pannus, synovitis, cartilage and bone destruction) and reduced inflammatory gene expression (IL-1β, IL-6, COX2). Further, this study also revealed that arthritis symptoms did not recur upon withdrawal of SD-282 treatment from mice treated at an early stage of disease.

Although several interventions have shown utility in early stage CIA in mice and in human RA, control of bone and cartilage destruction of the sort seen in advanced CIA in mice is the most challenging objective in the treatment of human RA. Several lines of evidence demonstrate that murine CIA progresses to an advanced state that is comparable

to that seen in humans. In areas of tumor-like synovial tissue, erosion of trabecular and cortical bone is common, leading to the characteristic erosions seen on radiography. In our model, osteoclasts can be seen in the areas of bone destruction during CIA. Furthermore, in patients with rheumatoid arthritis, elevated serum COMP levels are an important marker of cartilage degradation, and treatment with TNFα inhibitors, (infliximab or etanercept) have been shown to reduce COMP levels (Larsson *et al.*,1997, Joosten *et al.*,1999b and Crnkic *et al.*,2003). We detected elevated COMP levels in vehicle-treated over naïve mice.

Here, we report for the first time an oral, α-specific inhibitor of p38MAPK effective in the treatment of advanced CIA in mice. SD-282 treatment of mice with advanced arthritis resulted in significant improvement in clinical scoring and a decrease in paw swelling as compared to treatment with vehicle alone. Histological assessments comparing SD-282 and vehicle treatment cohorts revealed statistically significant results consistent with an interpretation of striking reversal in all aspects of joint disease, including reduced osteoclast number, synovitis, pannus, fibroplasia, an increase in joint space and decreased erosions in bone and cartilage (Figure 7, 8 and 9). The interpretation of positive reversal effects of SD-282 treatment on bone were also supported by improved bone parameters measured by μCT, including bone volume index, structural thickness and structural separation (Figure 6A and B, Table II). In addition, the improvement in cartilage in the SD-282 treatment group was accompanied by significant reduction in COMP levels.

It is well-established that p38αMAPK regulates key pro-inflammatory molecules in RA, including TNFα , IL-1β, IL-6 and COX 2. In the present study we have shown that, in animals with advanced disease, IL-1β, IL-6 and COX2 are prominent in the joint lesion and their expression is reduced with p38αMAPK inhibitor treatment. Using the same mouse arthritis model employed here, Joosten *et al.*(1996) demonstrated that anti-TNFα treatment had no beneficial effect in animals with advanced disease, suggesting this cytokine is less important in advanced stage of the disease in this model. This is consistent with our observation that TNFα expression in the joint was not elevated in animals with advanced disease when compared to naïve healthy mice. It is generally believed that TNFα is important in early stages of this disease model (Williams, *et al.*, 1992, Wooley, *et al.*,1993) but not in advanced disease (Joosten, *et al.*, 1996). IL-6 has been shown to be associated bone resorption (Palmqvist, *et al.*,2002) more precisely osteoclastogenesis (Li *et al., 2*004) and its inhibition reduces bone resorption (Suzuki *et al., 1*998 and Nishikawa *et al., 2*003). IL-1β blockade prevents cartilage and bone destruction in mouse CIA arthritis, whereas TNFα blockade only ameliorates joint inflammation (Joosten *et al.*, 1999a). Inhibition of COX-2 has been associated with reduced cartilage and bone destruction in rat adjuvant induced arthritis, suggesting that this enzyme is important for regulating disease progression (Chan *et al.*, 1999). Thus, effects on IL-6, IL-1β and COX-2 may alter the balance between osteolysis and osteogenesis in animals with advanced experimental arthritis.

Interestingly, these studies demonstrate that in a model of advanced arthritis associated with significant osteolysis, inhibition of p38αMAPK correlates with statistically

significant reversal of cartilage and bone destruction. A comparison of histology from arthritic animals in the baseline group and the SD-282 treatment group shows a striking improvement in bone density and cartilage integrity, suggesting not only a reversal but also a bone healing effect . Bone healing is also evidenced by significantly improved quantitative bone erosion scores between the baseline and SD-282 drug treatment groups. Erosion scores in the vehicle treatment group were even greater than those from the baseline group, suggesting bone erosion progresses in the absence of pharmacological intervention. The histological improvement in cartilage seen in the SD-282 group compared to baseline suggests that, in addition to reversing the disease, SD-282 also have a positive effect on bone and cartilage healing.

It appears that this bone healing could be achieved through a mechanism involving both bone resorption/osteoclastogenesis and bone formation/osteoblastogenesis. Available literature clearly indicate that p38MAPK is a potent mediator of osteoclastogeneis and osteoclast differentiation mediated by a wide variety of inducers including TNFα, RANKL and PGE2 (Nishikawa *et al., 2*003 and Steeve *et al., 2*004). p38MAPK inhibition has been shown previously to block bone resorption in fetal rat long bones *in vitro* (Kumar *et al.,* 2001). In the study reported here, inhibition of p38αMAPK was associated with reduced osteoclasts. It is doubtful, however, that this was sufficient to explain the extent of bone healing seen. Along with osteoclasts, other cell types (synovial fibroblasts and macrophages) produce enzymes and factors that could contribute to bone erosion. In mice with advanced arthritis, we noted reduced synovitis and reduced osteoclast numbers in the vehicle treatment group as compared to baseline; however,

joint space narrowing and bone and cartilage destruction was not reduced. In fact, by quantitative μCT, bone erosion scores continued to progress in the vehicle treated group but not in the SD-282 treated group. Indeed, by Day 61, erosion scores for the SD-282 treatment group achieved a level between those seen in the naïve (non-arthritic mice) and the baseline (start of therapy) group. This suggests that SD-282 healed bones in the late stage of CIA disease by reducing bone resorption and by forming new bone. We hypothesize that the effect of SD-282 on bone may be due to inhibition of osteoclast differentiation in the absence of IL-6 (Yamamoto et.al, 2003, Li et al., 2002 and Li et al., 2003) or/and osteoblastogenesis. We are in the process of testing the latter hypothesis. The effects on the cartilage may be due to inhibition of signaling cascades that mediate the up-regulation of COX-2 expression and PGE2 production in chondrocytes exposed to the pro-inflammatory cytokine IL-1beta and/or elevation of Col2A1 gene expression in the absence of IL-1 beta (Goldring and Berenbaum, 1999; and Nieminen et.al., 2005) . The loss of pannus tissue is a striking feature of SD-282 treatment. The exact mechanism resulting in this effect is not known. However, pro-inflammatory pathways are believed to promote the expansion and maintenance of pannus tissue (Desmoulins et al., 1990 and Paleolog et.al 1998). In this regard, the anti-inflammatory actions of p38 MAPK inhibition probably contribute to the effect on pannus noted in these studies. Further studies on the role of SD-282 in new bone formation with an aid of histomorphometry are warranted.

The present study indicates that inhibiting p38αMAPK during advanced stages of

murine collagen-induced arthritis improves all aspects of the disease including synovitis, joint space narrowing, and bone and cartilage structures. The inhibition of osteolytic lesions and reversal of cartilage and bone destruction reported in this model reflects the modulation of multiple p38αMAPK-dependent pathways including IL-1β, IL-6 and COX2. Thus, these studies suggest that inhibition of p38αMAPK has the potential to offer a unique therapeutic strategy for treating advanced stages of RA.

REFERENCES

Badger AM, Bradbeer JN, Votta B, Lee JC, Adams JL and Griswold DE (1996) Pharmacological profile of SB 203580, a selective inhibitor of cytokine suppressive binding protein/p38 kinase, in animal models of arthritis, bone resorption, endotoxin shock and immune function. *J. Pharmacol. Exp. Ther*. **279**: 1453-1461.

Chan CC, Boyce S, Brideau C, Charleson S, Cromlish W, Ethier D, Evans J, Ford-Hutchinson AW, Forrest MJU, Gauthier JY, Gordon R, Gresser M, Guay J, Kargman, S, Kennedy B, Leblanc Y, Leger S, Mancini J, O'Neill GP, Ouellet M, Patrick D, Percival MD Peprier H, Prasit P, Rodger I, Tagari P, Therien M, Vickers P, Visco D, Wang Z, Webb J, Wong E, Xu L-J, Yojng RN, Zamboni R and Riendeau D (1999) Rofecoxib (Vioxx, MK-0966; 4(4-methylsulfonylphenyl)-3phenyl-2-(5H)-furanone): A potent and orally active cyclooxygenase-2 inhibitor. Pharmacological and biochemical profiles. *J. Pharmacol. Exp. Therap.* **290**: 551-560.

Clerk A and Sugden PH (1998) The p38-MAPK inhibitor, SB203580, inhibits cardiac stress-activated protein kinases/c-Jun N-terminal Kinases (SAPKs/JNKs). *FEBS* **426**: 93 ~ 96

Crnkic M, Mansson B, Larsson L, Geborek P, Heinergard D and Saxne T (2003) Serum cartilage oligomeric matrix protein (COMP) decreased in rheumatoid arthritis

patients treated with infliximab or etanercept. *Arthritis Research and Therapy* **5**: 181-185.

Desmoulins D, Ponteziere C, Agneray J, Ekindjian OG and Cals MJ (1990) Effects of human recombinant IL-1 beta on rheumatoid and non-rheumatoid human synovial cell growth. *Cell Mol Bio* **36**: 309-316.

Genant HK, Jiang Y, Peterfy C, Lu Y, Redei J and Countryman P (1998) Assessment of rheumatoid arthritis using a modified scoring method on digitized and original radiographs. *Arthritis Rheum.* **41**:1583-1590.

Goedert M, Cuenda A, Craxton M, Jakes R and Cohen P (1997) Activation of the novel stress-activated protein kinase SAPK4 by cytokines and cellular stresses is mediated by SKK3 (MKK6); comparison of its substrate specificity with that of other SAP kinases. *EMBO J.* **16:** 3563–3571.

Goldring MB and Berenbaum F (1999). Human chondrocyte culture models for studing cyclooxygenase expression and prostaglandin regulation of collagen gene expression. Osteoarthritis Cartilage 7: 386-388.

Jiang Y, Zhao J, White DL and Genant HK (2000) Micro CT and micro MR imaging of 3D architecture of animal skeleton. *J. Musculoskel. Neuron Interact.* 1: 45-51.

Jiang Y, Zhao J and Genant HK (2002) Macro and Micro Imaging of Bone Architecture. *In* Principles of Bone Biology, 2nd edition. J.P. Bilezikian, L.G. Raisz, and G.A. Rodan editors. Academic Press. San Diego, CA. 1599-1623.

Jiang Y, Zhao J, Mitlak BH, Wang O, Genant HK and Eriksen EF (2005) Recombinant human parathyroid hormone (1-34) [Teriparatide] Improves both cortical and cancellous bone structure. *J. Bone Miner. Res.* (In press)

Joosten LAB, Helsen MA, and Berg WB (1994) Accelerated onset of collagen-induced arthritis by remote inflammation. *Clin.Exp.Immunol.* 97: 204-211.

Joosten LA, Helsen MM, van de Loo FA and van den Berg WB (1996) Anticytokine treatment of established type II collagen-induced arthritis in DBA/1 mice. A comparative study using anti-TNF alpha, anti-IL-1 alpha/beta, and IL-1Ra. *Arthritis Rheum*. **39**: 797-809.

Joosten LAB, Lubberts E, Helsen MMA and van den Berg WB (1997) Dual role of IL-12 in early and late stages of murine collagen type II arthritis. *J. Immunol.* **159**: 4094-4102.

Joosten LAB, Helsen MMA, SaxneT, Loo FAJ, Heinegard D and Berg WB (1999a) IL-1αβ blockade prevents cartilage and bone destruction in murine type II collagen-

induced arthritis, whereas TNF alpha blockade only ameliorates joint inflammation. *J. Immunology* **80**:5049-5055

Joosten LAB, Lubberts E, Helsen MMA, Saxne T, Roo CJJC, Heinegard D and van den Berg WB (1999b) Protection against cartilage and bone destruction by systemic interleukin-4 treatment in established murine type II collagen induced arthritis. *Arthritis Research* **1**: 81-91.

Hale KK., Trollinger D, Rihanek M and Manthey CL (1999) Differential Expression and Activation of p38 Mitogen-Activated Protein Kinase α**,** β**,**γ**,** and δ in Inflammatory Cell Lineages *J. Immunol.* **162:** 4246 - 4252.

Kumar S, Boehm J and Lee JC (2003) p38 MAP kinase: key signaling molecules as therapeutic target for inflammatory diseases. *Nat. Rev. Drug. Discov.* **9**: 717-726.

Kumar S, Votta BJ, Rieman DJ, Badger AM, Gowen M and Lee JC. (2001) IL-1 and TNF-induced bone resorption is mediated by p38 mitogen activated protein kinase. *J. Cell. Physiol.* **187**: 294-303.

Kumar S, McDonnell PC, Gum R J and Hand AT (1997) Novel homologues of CSBP/p38 MAP kinase: activation, substrate specificity and sensitivity to inhibition by pyridinyl imidazoles. *Biochemical and Biophysical Research Comm*. **235:** 533-538.

Larsson E, Mussener A, Heinegard D, Klareskog L and Saxne T (1997) Increased serum levels of cartilage oligomeric matrix protein and bone sialoprotein in rats with collagen arthritis. *Br. J. Rheumatol.* **36**:1258-1261.

Li X, Udagawa N, Itoh K, Suda K, Murase Y, Nishihara T, Suda T and Takashashi N (2002) P38 MAPK-mediated signals are required for inducing osteoclasts differentiation but not for osteoclast function. *Endocrinology* **143**:3105-3113.

Li X, Udagawa N, Takami M, Sato N, Kobayashi Y and Takahashi N (2003). P38 Mitogen-activated protein kinase is crucially involved in osteoclast differentiation but not in cytokine production, phagocytosis, or dendritic cell differentiation of bone marrow macrophages. *Endocrinology* **144**: 4999-5005.

Li Z, Tran TT, Ma JY, O'Young G, Kapoun AM, Chakravarty S, Dugar S, Schreiner G and Protter AA (2004) p38 alpha mitogen-activated protein kinase inhibition improves cardiac function and reduces myocardial damage in isoproterenol-induced acute myocardial injury in rats. *J Cardiovasc Pharmacol.* **44**:486-492.

McLay LM, Halley F, Souness JE, McKenna J, Benning V, Birrell M, Burton B, Belvisi M, Collis A Constan A, Foster M, Hele D, Jayyosi Z, Kelley M, Maslen C, Miller G, Ouldelhkim MC, Page K, Phipps S, Pollock K, Porter B, Ratcliffe AJ, Redford EJ, Webber S, Slater B, Thybaud V and Wilsher N (2001) The discovery

of RPR 200765A, a p38 MAP kinase inhibitor displaying a good oral anti-arthritic efficacy. *Bioorg Med Chem.* **9**:537-554.

Nieminen R, Leinonen S, Lahti A, Vuolteenaho K, Jalonen U, Kankaanranta H, Goldring MB and Moilanen E (2005). Inhibitors of mitogen-activated protein kinases downregulate COX-2 expression in human chondrocytes. *Mediators Inflamm,* **2005**: 249-255.

Nishikawa M, MyouiA, Tomita T, Takashi K, Nampei A and Yoshikawa H (2003) Prevention of the onset and progression of collagen-induced arthritis in rats by the potent p38 mitogen-activated protein kinase inhibitor FR167653. *Arthritis Rheum.* **48**: 2670-2681.

Palmqvist, P, Persson E, Conaway HH and Lerner UH (2002) IL-6 Leukemia inhibitory factor, and oncosatin M stimulate bone resorption and regulate the expression of receptor activator of NF-kB ligand, osteoprotegerin, and receptor activator of NF-kB in mouse calvariae. *J. Immunology* **169**: 3353-3362.

Paleolog EM, Young S, Stark AC, McCloskey RV, Feldman M and Maini RN (1998). Modulation of angiogenic vascular endothelial growth factor by tumor necrosis factor alpha and interleukin-1 in rheumatoid arthritis. *Arthritis Rheum* **41**: 1258-1265.

Parfitt AM (1983) The sterologic basis of bone histomorphometry. Theory of quantitative microscopy and reconstruction of the third dimension. *In* Bone Histomorphometry. Techniques and Interpretations. R. Recker, editor. CRC Press, Boca Raton, FL. 53-87.

Rioja I., Bush KA, Buckton JB, Dickson MC and Life PF (2004) Joint cytokine quantification in two rodent arthritis models: kinetics of expression, correlation of mRNA and protein levels and response to prednisolone treatment. *Clin Exp Immunol.* **137**:65–73.

Saxne T and D Heinegard (1992) Cartilage oligomeric matrix protein: a novel marker of cartilage turnover detectable in synovial fluid and blood. *Br. J. Rheum.* **31**: 583-591.

Steeve KT, Marc P, Sandrine T, Dominique H and Yannick F (2004) IL-5, RANKL, TNF-alpha/Il-1: interrelations in bone resorption pathophysiology. *Cytokine and Growth Factor Reviews* **15**: 49-60.

Suzuki Y, Nishikaku F, Nakatuka M and Koga Y (1998) Osteoclast-like cells in murine collagen induced arthritis. *J. Rheumatology* **25**: 1154-1160.

Sweitzer SM, Medicherla S, Almirez R, Dugar S, Chakravarty S, Shumilla JA, Yeomans DC and Protter AA (2004) Antinociceptive action of a p38alpha MAPK inhibitor, SD-282, in a diabetic neuropathy model. *Pain.* **109**:409-419.

Takeshita S, Namba N, Zhao J, Jiang Y, Genant HK, Silva MJ, Brodt MD, Helgason CD, Kalesnikoff J, Rauh MJ, Humphries RK, Krystal G, Teitelbaum SL and Ross FP (2002) SHIP-deficient mice are severely osteoporotic due to increased numbers of hyper-resorptive osteoclasts. *Nature Medicine* **8**:943-949.

Vingsbo-Lunderg C, Saxne H, Olsson H and Holmdahl R (1998). Increased serum levels of cartilage oligomeric matrix protein chronic erosive arthritis in rats. *Arthritis Rheum.* **41**:544-550

Williams RO, Feldmann M and Maini RN (1992) Anti-tumor necrosis factor ameliorates joint disease in murine collagen-induced arthritis. *Proc. Natl. Acad. Sci.* USA **89**: 9784 -9788.

Wooley PH, Dutcher HJ, Widmer MB and Gilles S (1993) Influence of a recombinant human soluble tumor necrosis factor receptor FC fusion protein on type II collagen-induced arthritis in mice. *J. Immunol.* **151**:6602-6607.

Yamamoto A, Fukuda A, Seto H, Mivazaki T, Kadono Y, Sawada y, Nakamura I, Katagiri H, Asano T, Tanaka Y, Oda H, Nakamura K and Tanaka S (2003).

Suppression of arthritic bone destruction by adenovirus-mediated dominant-negative Ras gene transfer to synoviocytes and osteoclasts. *Arthritis Rheum*, **48**: 2682-2692.

FIGURE LEGENDS

Figure 1: Phosphorylated p38MAPK in paws from naïve mice and mice with CIA: p38MAPK is phosphorylated and activated in arthritic mice. Whole mouse paw extracts (20 μg/lane) were subjected to SDS-PAGE and immunoblot analysis. Blots were probed with anti-phospho p38 and anti-p38MAPK antibodies. Immunodetection was visualized by ECL. Each lane represents inflamed paw lysate from a single animal. Results are representative of one experiment, and a total of 5 arthritic and 3 naïve mice.

Figure 2. Treatment with SD-282 improves clinical severity scores in mice with early CIA disease. Mice with early stage CIA were divided into three groups each of 15 mice. Groups were treated by oral gavage twice daily with vehicle (open circles) or SD-282, 30 mg/kg (open triangles) or 90 mg/kg (filled circles) for 10 days. Values are reported as the mean ± SD. *$p<0.05$, **$p<0.001$ versus vehicle, by non-parametric Bonferroni multiple comparison test. SD-282 reduced clinical severity scores in a dose-dependent manner.

Figure 3: Treatment with SD-282 inhibits IL-6, IL-1β and COX-2 mRNA induction in arthritic paws of mice with early CIA disease. Taqman analysis of inflamed mouse paw tissues. Values are reported as the mean ± SD. Note the diminished mRNA expression of IL-6 (*$p<0.04$ versus vehicle by two tailed t test; A), IL-1β (*$p<0.05$ versus vehicle by two tailed t test; B) and COX-2 (*$p<0.005$ versus vehicle by two tailed t test; C)

Figure 4: Treatment with SD-282 ameliorates cartilage and bone loss in mice with early CIA disease. Note normal bone joint in naïve group (A), severe inflammation, cartilage and bone destruction in vehicle group (B1 and B2), and reduced inflammation and ameliorated cartilage and bone pathology in SD-282 at 90 mg/kg group (C).

Figure 5: Treatment with SD-282 improves clinical disease scores in mice with advanced CIA disease. Mice with advanced CIA (30 days after immunization) were divided into three groups each of 12 mice. Groups were treated by oral gavage twice daily with vehicle (open circles) or SD-282, 30 mg/kg (open triangles) or 90 mg/kg (hatched circles) for 20 days. Values are reported as the mean ± SD. *$p<0.05$, **$p<0.001$versus vehicle, calculated by non-parametric Bonferroni multiple comparison test. SD-282 significantly reduced clinical severity scores in a dose-dependent manner.

Figure 6: 3-dimentional uCT reconstructions of the rear paws showing that SD 282 reverses bone erosion. The cortical bone and articular surface of the metatarsals I to V, the cuneiforms I to III, the cuboid, the navicular, the calcaneus, the talus, the distal fibula, and the distal tibia can be observed in these images. There are severe erosions in all the bones in the right paw from the vehicle group (Figure 6A). No erosion can be observed in the paw from the group receiving treatment with 90 mg/kg SD-282 (Figure 6B).

Figure 7: SD-282 reverses cartilage and bone loss and promotes bone healing in mice with advanced CIA. SD-282 treatment improves histological scoring. Mice showing signs of advanced disease on Day 33 were randomized to three groups: (1) baseline animals, sacrificed on day 33, (2) 28-day vehicle treatment, sacrificed on Day 61 and (3) 28-day treatment with SD-282 at 90 mg/kg, sacrificed on Day 61. Knee joint histology from representative naïve mice (A), baseline on Day 33 (B), and treatment at Day 61 with vehicle (C) and SD-282 at 90 mg/kg (D) are shown. Knee joint histology of vehicle treated mice on Day 61 reveals severe bone and cartilage destruction, pannus accumulation, neutrophil and macrophage (ED-1 staining) infiltration. Histology from the SD-282 treatment group at Day 61 (D) reveals marked improvement in joint histology including evidence of cartilage and bone healing.

Figure 8: SD-282 reverses cartilage, bone and joint destruction as well as synovitis, pannus and fibroplasia in mice with advanced CIA. Mice showing signs of advanced disease were selected 33 days after initial collagen immunization and divided into three groups. One group (baseline) was sacrificed on day 33. The other two groups were treated with vehicle or SD-282 at 90 mg/kg daily until Day 61. Open bars are histopathology scores of paws from baseline i.e., Day 33; hatched black bars show scores of paws from the vehicle-treated group at Day 61, and hatched gray bars show scores of paws from SD-282 at 90 mg/kg treated group at Day 61. SD-282 significantly reduces cartilage erosion (**$p<0.01$), bone erosion (*$p<0.05$), joint destruction

(***p<0.001), synovitis (**p<0.01), pannus (***p<0.0001) and fibroplasia (**p<0.01) when compared to the vehicle-treated group. Values are reported as the mean ± SD. Statistics were calculated by non-parametric Bonferroni multiple comparison test.

Figure 9: SD-282 reduces osteoclast number in mice with advanced CIA. Note arrows in the Figure A1 and A2 of vehicle treated group for abundant osteoclasts. SD-282 treatment (B1 and B2) almost removed those osteoclasts in joint tissue from CIA mice with advanced disease on day 61.

Figure 10: SD-282 reduces IL-1β, IL-6 and COX-2 expression in inflamed joints in mice with advanced CIA. Mice with joint histology showing signs of advanced disease on Day 33 were randomized to three groups: (column A) baseline animals, sacrificed on Day 33, (column B) 28-day vehicle treatment, sacrificed on Day 61 and (column C) 28-day treatment with 90 mg/kg SD-282, sacrificed on Day 61. Sections were probed for expression of IL-1β (row 1), IL-6 (row 2) and COX-2 (row 3) in the pannus of synovium and in the chondrocytes of cartilage by immunohistochemistry. SD-282 treatment at Day 61 was associated with marked reduction of IL-1β (C1), IL-6 (C2) and COX-2 (C3) expression when compared to the corresponding vehicle groups (B1, B2 and B3) as well as baseline groups (A1, A2 and A3).

JPET Fast Forward. Published on April 5, 2006 as DOI: 10.1124/jpet.105.098020
This article has not been copyedited and formatted. The final version may differ from this version.

Table I. Specificity of SD-282 for p38 MAPK isoforms

Kinase Target	IC_{50} (μmol/L)	
	SD-282	Control
p38α	0.00161	0.022*
p38β	0.023	0.028*
p38γ	>10uM	0.57**
p38δ	>10uM	0.36**

* SB 202190. **Staurosporine

JPET Fast Forward. Published on April 5, 2006 as DOI: 10.1124/jpet.105.098020
This article has not been copyedited and formatted. The final version may differ from this version.

Table II. SD-282 reverses bone destruction as evidenced by bone volume, thickness and separation

	BV/TV	Thickness (mm)	Separation (mm)
Vehicle	0.41 ± 0.1	0.13 ± 0.3	0.27 ± 0.04
SD292, 90 mg/kg	0.74 ± 0.05	0.22 ± 0.1	0.20 ± 0.05
p-value	<0.009	<0.009	0.047

JPET Fast Forward. Published on April 5, 2006 as DOI: 10.1124/jpet.105.098020
This article has not been copyedited and formatted. The final version may differ from this version.

Table III. SD-282 lowers COX-2, IL-β and Il-6 expression in the joint tissue of CIA mice with advanced disease

Groups	Scoring for Immunohistochemical staining (Mean±SD)		
	COX-2	IL-1β	IL-6
Naïve (n = 3)	0	0	0
Baseline (n = 6)	2.58 ± 0.74	3.0 ± 0.45	0.58 ± 0.66
Vehicle (n = 12)	2.67 ± 0.49	2.13 ± 1.11	3.42 ± 0.79
SD-282 at 90mg/kg (n = 12)	1.17 ± 1.25	0.88 ± 1.09	2.17 ± 1.34
p-value*	<0.01	<0.02	<0.007

*p-value for SD-282 treatment group compared to the vehicle group

JPET Fast Forward. Published on April 5, 2006 as DOI: 10.1124/jpet.105.098020
This article has not been copyedited and formatted. The final version may differ from this version.

Figure 1:

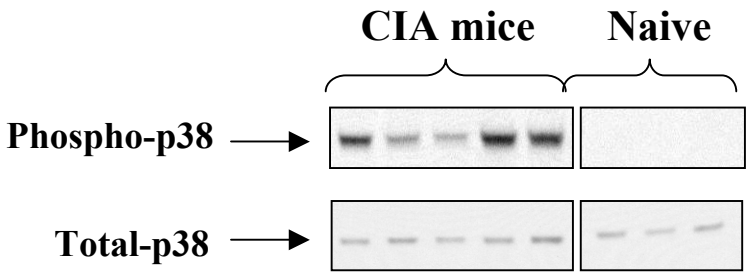

JPET Fast Forward. Published on April 5, 2006 as DOI: 10.1124/jpet.105.098020
This article has not been copyedited and formatted. The final version may differ from this version.

Figure 2:

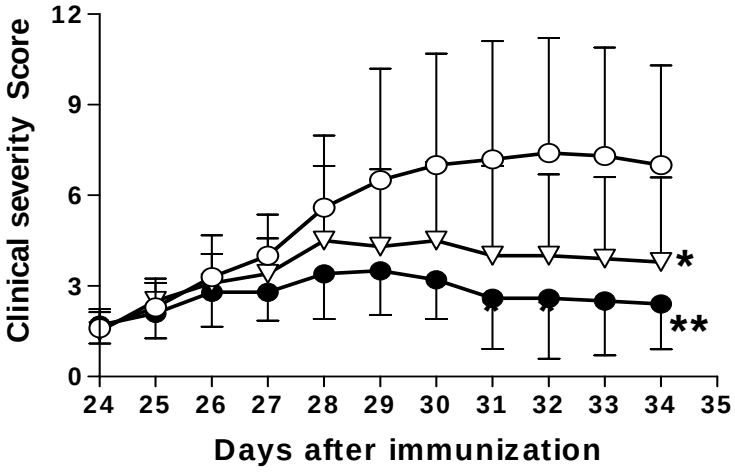

JPET Fast Forward. Published on April 5, 2006 as DOI: 10.1124/jpet.105.098020
This article has not been copyedited and formatted. The final version may differ from this version.

Figure 3:

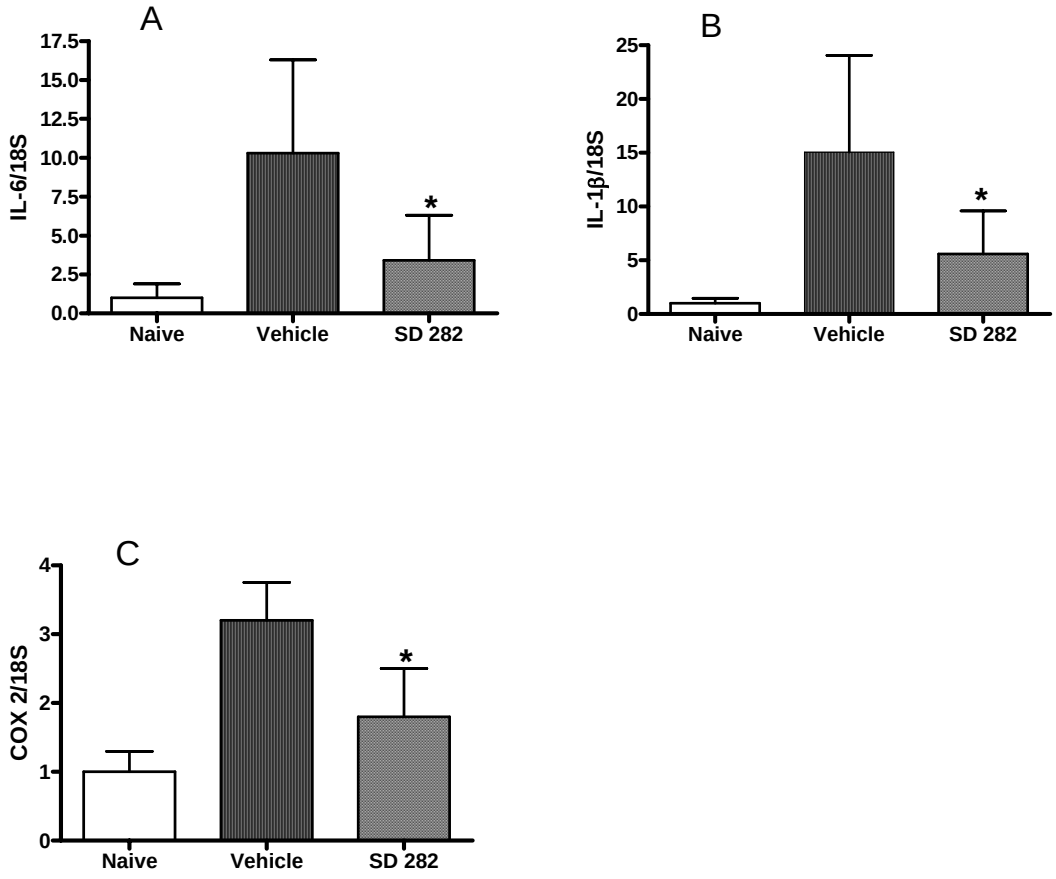

JPET Fast Forward. Published on April 5, 2006 as DOI: 10.1124/jpet.105.098020
This article has not been copyedited and formatted. The final version may differ from this version.

Figure 4:

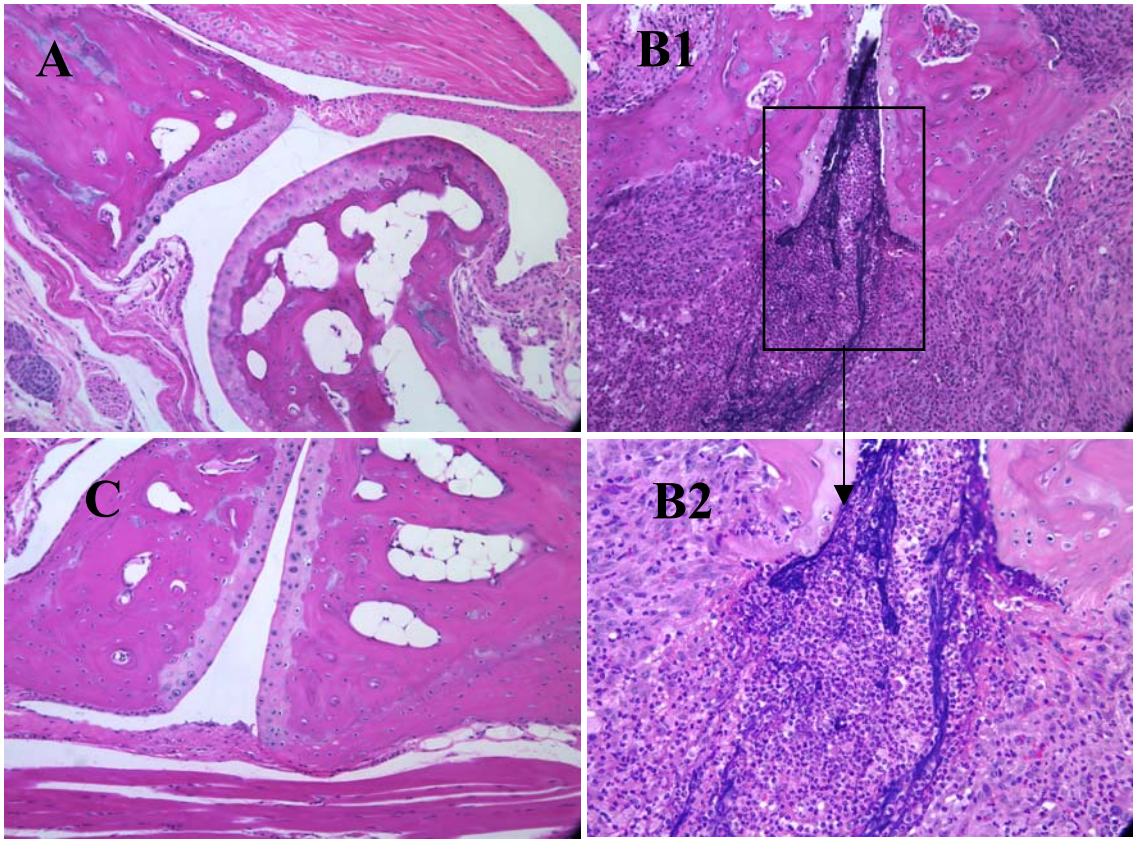

JPET Fast Forward. Published on April 5, 2006 as DOI: 10.1124/jpet.105.098020
This article has not been copyedited and formatted. The final version may differ from this version.

Figure 5:

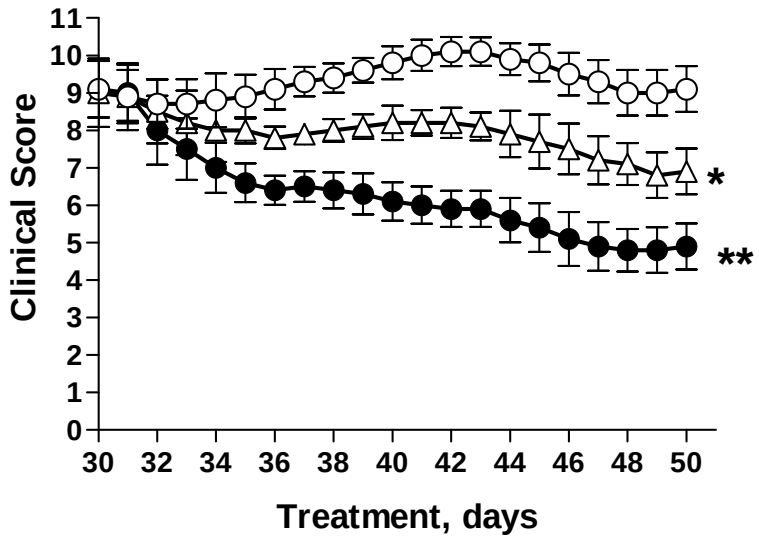

JPET Fast Forward. Published on April 5, 2006 as DOI: 10.1124/jpet.105.098020
This article has not been copyedited and formatted. The final version may differ from this version.

Figure 6:

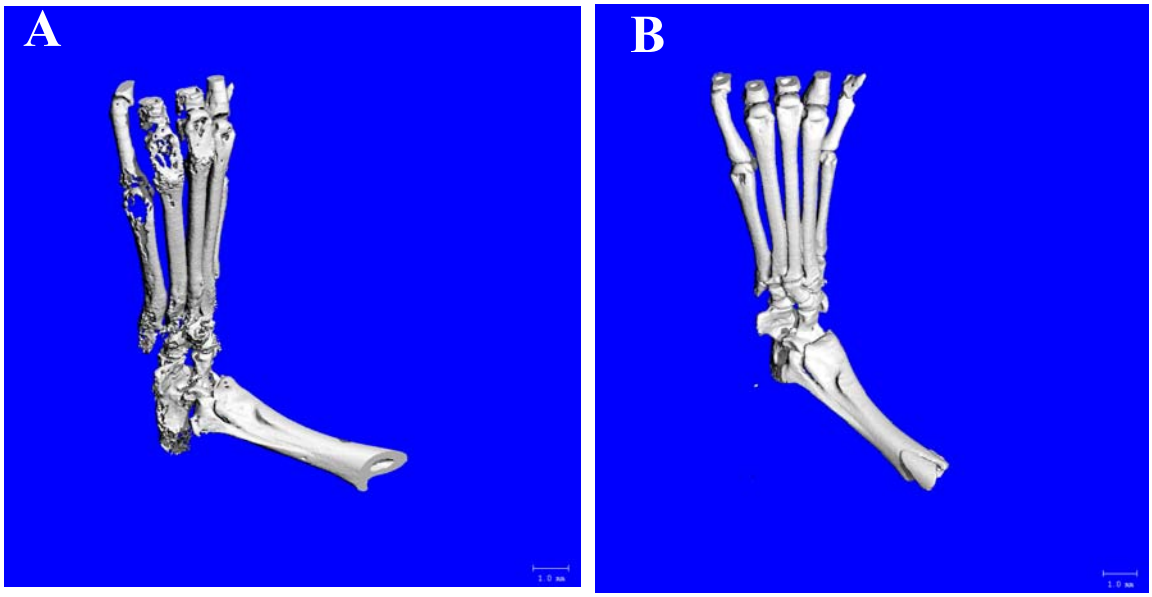

JPET Fast Forward. Published on April 5, 2006 as DOI: 10.1124/jpet.105.098020
This article has not been copyedited and formatted. The final version may differ from this version.

Figure 7:

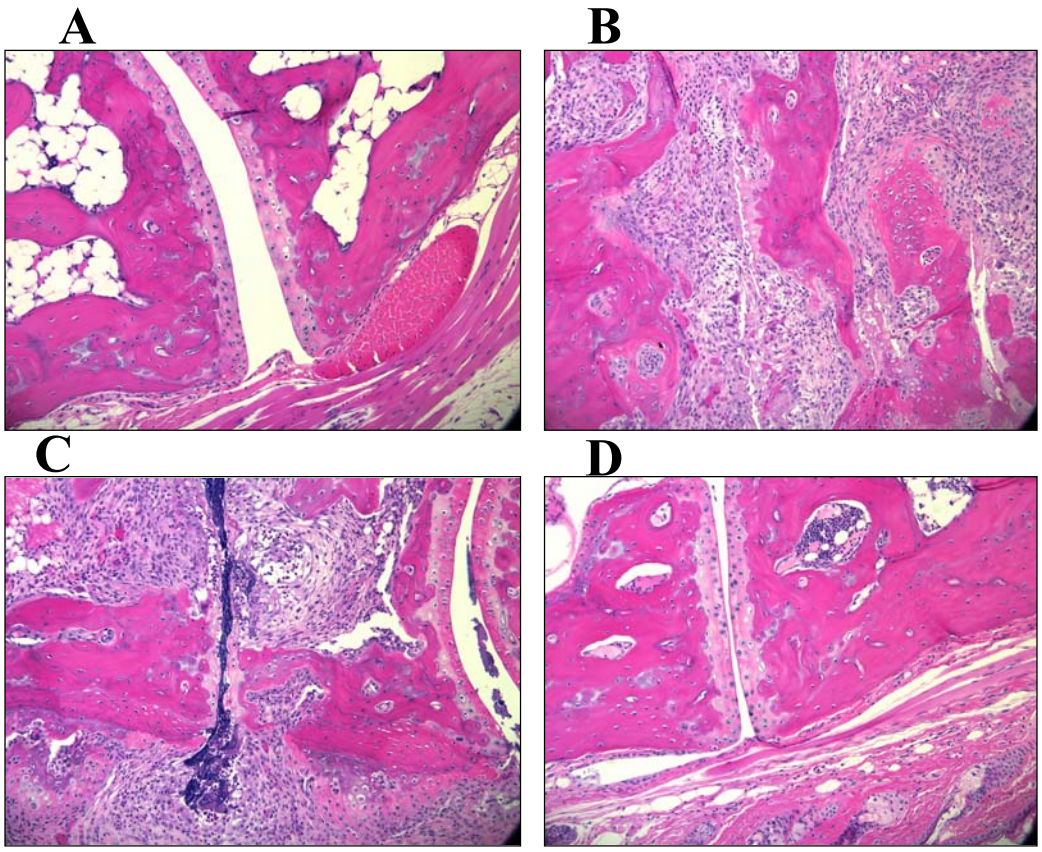

JPET Fast Forward. Published on April 5, 2006 as DOI: 10.1124/jpet.105.098020
This article has not been copyedited and formatted. The final version may differ from this version.

Figure 8:

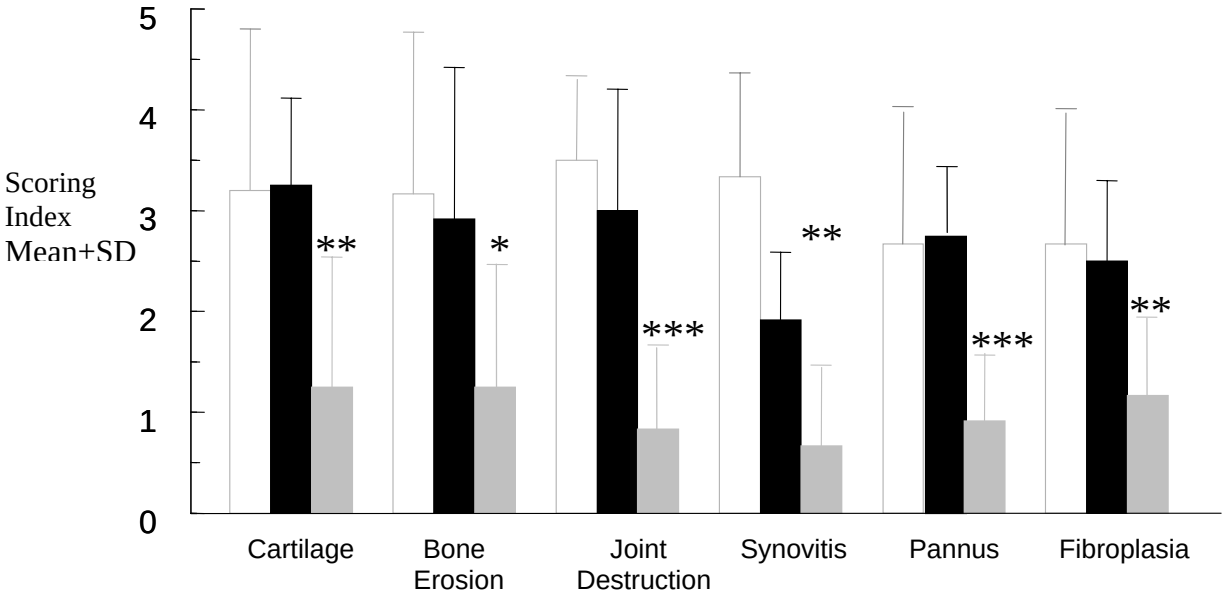

JPET Fast Forward. Published on April 5, 2006 as DOI: 10.1124/jpet.105.098020
This article has not been copyedited and formatted. The final version may differ from this version.

Figure 9:

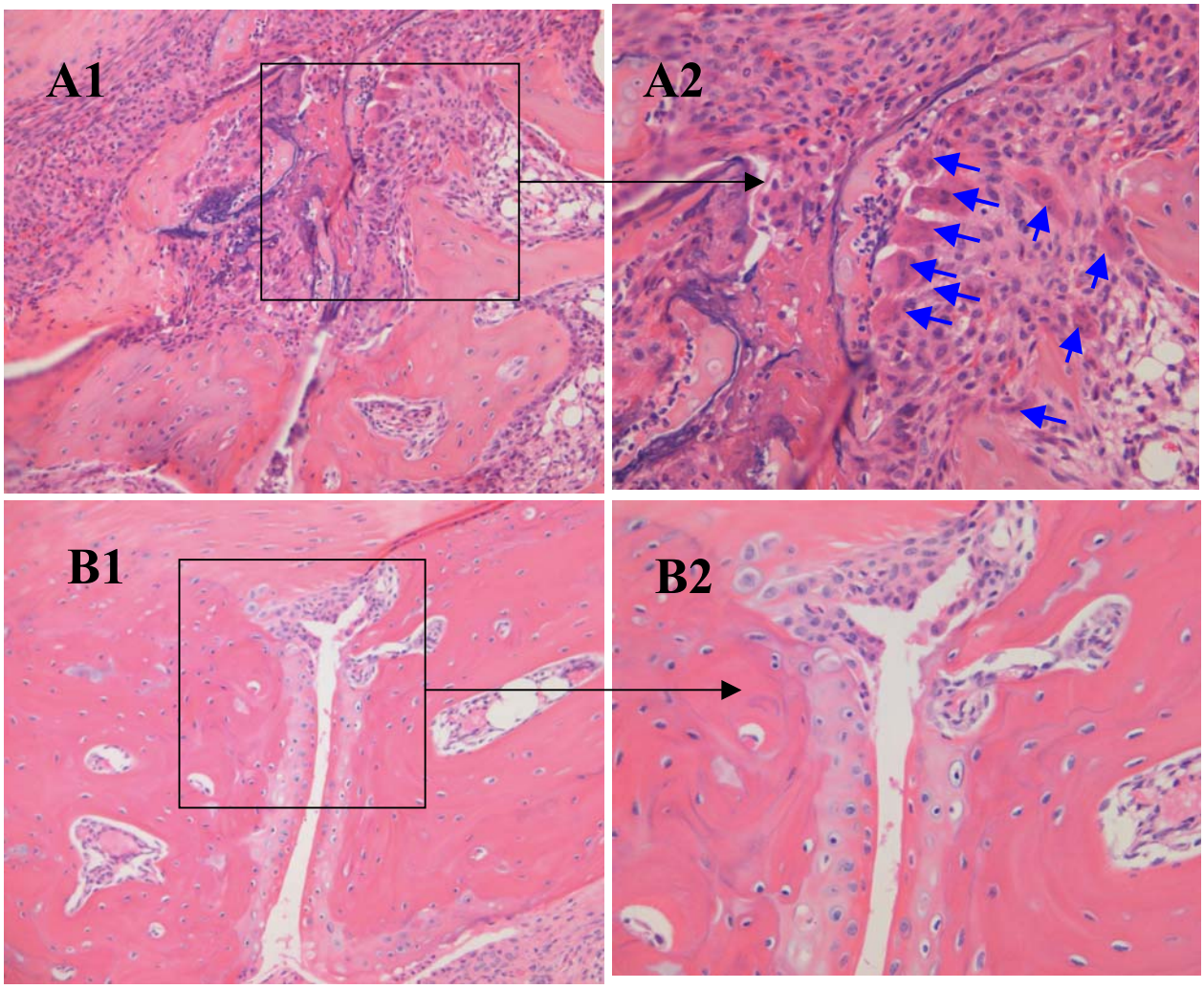

JPET Fast Forward. Published on April 5, 2006 as DOI: 10.1124/jpet.105.098020
This article has not been copyedited and formatted. The final version may differ from this version.

Figure 10: